

Satellites around massive galaxies since $z \sim 2$

E. Marmol-Queralto^{1,2*}, I. Trujillo^{1,2}, P.G. Perez-Gonzalez^{3,4}, J. Varela^{1,2,5} and G. Barro⁶

¹*Instituto de Astrofısica de Canarias, c/ Vıa Lactea s/n, E-38205, La Laguna, Tenerife, Spain*

²*Departamento de Astrofısica, Universidad de La Laguna, E-38205, La Laguna, Tenerife, Spain*

³*Departamento de Astrofısica, Facultad de CC. Fısicas, Universidad Complutense de Madrid, E-28040, Spain*

⁴*Associated Astronomer at Steward Observatory, The University of Arizona*

⁵*Centro de Estudios de Fısica del Cosmos de Aragon (CEFCA), Plaza San Juan, 1, Planta-2, E44001-Teruel, Spain*

⁶*UCO/Lick Observatory, University of California, Santa Cruz, CA 95064*

ABSTRACT

Accretion of minor satellites has been postulated as the most likely mechanism to explain the significant size evolution of the massive galaxies over cosmic time. Using a sample of 629 massive ($M_{\text{star}} \sim 10^{11} M_{\odot}$) galaxies from the near-infrared Palomar/DEEP-2 survey, we explore which fraction of these objects has satellites with $0.01 < M_{\text{sat}}/M_{\text{central}} < 1$ (1:100) up to $z = 1$ and which fraction has satellites with $0.1 < M_{\text{sat}}/M_{\text{central}} < 1$ (1:10) up to $z = 2$ within a projected radial distance of 100 kpc. We find that the fraction of massive galaxies with satellites, after the background correction, remains basically constant and close to 30% for satellites with a mass ratio down to 1:100 up to $z = 1$, and $\sim 15\%$ for satellites with a 1:10 mass ratio up to $z = 2$. The family of spheroid-like massive galaxies presents a 2-3 times larger fraction of objects with satellites than the group of disk-like massive galaxies. A crude estimation of the number of 1:3 mergers a massive spheroid-like galaxy experiences since $z \sim 2$ is around 2. For a disk-like galaxy this number decreases to ~ 1 .

Key words: galaxies: evolution – galaxies: high-redshift – galaxies:formation

1 INTRODUCTION

The relevance of major mergers as the main mechanism for the size increase of the massive ($M_{\text{star}} \gtrsim 10^{11} M_{\odot}$) galaxies in the last ~ 11 Gyr (e.g., Daddi et al. 2005; Trujillo et al. 2006, 2007; Longhetti et al. 2007; Buitrago et al. 2008) has been disfavored observationally (e.g., Bundy et al. 2009; de Ravel et al. 2009; Lopez-Sanjuan et al. 2010). This has left room to a growing consensus that the strong size evolution observed among the massive galaxies is mainly dominated by the continuous accretion of minor satellites. However, all the observational evidences compiled so far suggesting that the minor merging is the main route of galaxy size growth it is only indirect. The observations that favor the minor merging scenario are: a) a progressive build-up of the envelopes of the massive galaxies with cosmic time (Hopkins et al. 2009; Bezanson et al. 2009; van Dokkum & Brammer 2010; Carrasco et al. 2010) and b) a mild decrease in the velocity dispersion of these galaxies (e.g., Cenarro & Trujillo 2009; Cappellari et al. 2009; Martinez-Manso et al. 2011; Newman et al. 2010; van de Sande et al. 2011). Both phenomena agree with a process that do not affect dramatically their inner regions. Recently, an extra evidence supporting the merging scenario has been stated: the size evolution of the massive galaxies is not linked to the age of the stellar population of the galaxies (Trujillo et al. 2011). All

these observations disfavor the puffing-up mechanism proposed by Fan et al. (2008, 2010), where galaxies grow by the expulsion of gas by the AGN activity, and give support to the minor merging hypothesis.

On the theoretical side, N-body cosmological simulations as well as semianalytical models (e.g., Khochfar & Burkert 2006; Naab et al. 2009; Oser et al. 2011) show that the expected accretion rate of satellites should be able to produce a significant increase in the size of the galaxies while at the same time changing the velocity dispersion only mildly. Estimates of the merger rate (e.g., Lopez-Sanjuan et al. 2011) using observations are, however, not straightforward due to the large uncertainties in the determination of the merging timescales. Nevertheless, a more direct way of confronting simulations with observations and, consequently, probing the minor merging scenario is to measure the frequency of satellites found around massive galaxies and quantify how this fraction changes with cosmic time (e.g., Newman et al. 2011). Several papers have calculated this number in the nearby Universe (see e.g., Chen 2008; Liu et al. 2011). These works show that $\sim 12\%$ of the massive galaxies have at least a satellite with a stellar mass $0.1 < M_{\text{sat}}/M_{\text{central}} < 1$ within a projected radius of 100 kpc. These numbers are in very nice agreement with expectations from Λ CDM simulations (see e.g., Boylan-Kolchin et al. 2010). de Ravel et al. (2011) and Nierenberg et al. (2011) have explored the evolution of the fraction of galaxies with satellites up to $z \sim 1$ but using mostly samples of central galaxies less mas-

* E-mail: emq@iac.es

sive than $10^{11}M_{\odot}$. In this paper we concentrate on the most massive galaxies and we expand on the previous analysis exploring the fraction of galaxies with satellites up to $z \sim 2$. To reach our goal we use a large and complete sample of massive galaxies up to $z = 2$ from Trujillo et al. (2007). We probe two different redshift ranges: up to $z = 1$, we explore the fraction of massive galaxies with satellites having $0.01 < M_{\text{sat}}/M_{\text{central}} < 1$, and up to $z = 2$, the fraction of massive galaxies with satellites within the mass range $0.1 < M_{\text{sat}}/M_{\text{central}} < 1$.

This letter is structured as follows. In Section 4 we describe our sample of massive galaxies and the photometric catalog we have used for identifying their satellites. Our criteria for selecting satellites as well as our background estimation methods are explained in Section 3. Finally, our results are presented in Section 4, and a discussion of our findings is provided in Section 5. In this paper we adopt a standard Λ CDM cosmology, with $\Omega_m = 0.3$, $\Omega_{\Lambda} = 0.7$ and $H_0 = 70 \text{ km s}^{-1} \text{ Mpc}^{-1}$.

2 THE DATA

To analyse the evolution with redshift of the fraction of massive galaxies having satellites, we have used as the reference catalog for the central galaxies the compilation of massive objects published in Trujillo et al. (2007) (hereafter T07). This is a homogeneous and large collection of massive galaxies since $z = 2$. Briefly, the sample consists on a total of 831 massive ($M_{\text{star}} > 10^{11}M_{\odot}$) galaxies (of which 35 were identified as AGN and not used onwards) over 710 arcmin^2 in the Extended Groth Strip (EGS). These objects were K_s -band selected in the Palomar Observatory Wide-Field Infrared (POWIR)/DEEP-2 survey (Bundy et al. 2006; Conselice et al. 2007). In total, 372 galaxies have spectroscopic redshifts (Davis et al. 2003), whereas the remaining redshifts were obtained photometrically using B, R and I bands from the CFHT 3.6m-telescope, F606W and F814W from the Hubble Space Telescope and J and K_s from the Palomar 5-m telescope. Stellar masses and other derived photometric parameters were estimated using a Chabrier (Chabrier 2003) initial mass function (IMF). T07 estimated (circularized) half-light radius (r_e) and Sérsic indices n (Sérsic 1968) for all the galaxies in our sample.

To compile the sample of the satellite galaxies around our massive objects we have used the EGS IRAC-selected galaxy sample from the Rainbow Cosmological Database¹ published by Barro et al. (2011a) (see also Pérez-González et al. 2008). This database covers an area of 1728 arcmin^2 centred on the EGS and provides spectral energy distributions (SEDs) ranging from the UV to the MIR regime plus well-calibrated and reliable photometric redshifts and stellar masses (Barro et al. 2011b). Around 10% of the galaxies in the Rainbow catalogue have spectroscopic redshifts. From the Rainbow database we have selected all the galaxies with $z < 2.2$ and an estimated stellar mass $10^8 M_{\odot} < M < 10^{12} M_{\odot}$. A total of ~ 55000 objects were selected in the EGS area following these criteria. We refer to this resulting sample as the Rainbow catalog.

The sample of massive galaxies as well as the Rainbow sample were cross-correlated using a $1.0''$ search radius to create a sample of central galaxies identified in both catalogs. All the massive galaxies in T07 were found in the Rainbow database. The average difference between the photometric redshifts for the massive galaxies in both samples is $\sim 10\%$. The average stellar mass of our

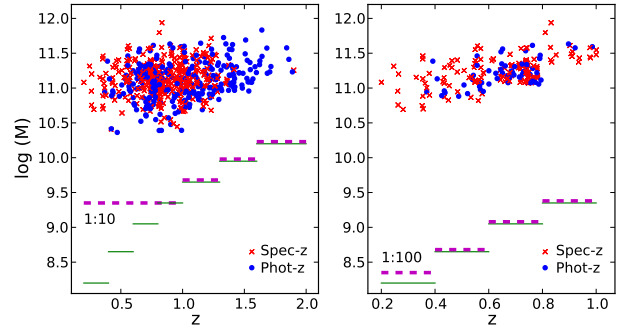


Figure 1. Stellar mass vs. redshift for the massive galaxies analysed in this work. Galaxies with spectroscopic redshifts are plotted in red, while galaxies with photometric estimates are plotted in blue. The left panel shows the distribution of the massive galaxies used selected for exploring the fraction of galaxies with 1:10 satellites up to $z = 2$. The right panel shows the massive galaxies used in the study of 1:100 satellites up to $z = 1$. The solid green lines illustrate the stellar mass 75% completeness limit of the Rainbow database for the redshift ranges given in Barro et al. (2011b). The magenta dashed lines the stellar mass cut used in this paper for the different subsamples.

massive sample according to the Rainbow dataset is $0.9 \times 10^{11} M_{\odot}$ and $1.7 \times 10^{11} M_{\odot}$ according to T07.

In order to build a sample of central galaxies with the best estimations of redshifts and stellar masses we have applied the following rules: a) if a central galaxy has a spectroscopic redshift determination in Rainbow (348 objects), we have used this redshift plus the stellar mass inferred in that catalog for these two quantities. Among these galaxies, there were 8 objects with spectroscopic redshifts in both samples with high discrepancies in the stellar mass estimations from both catalogs. We reject from our sample such dubious cases. b) If no spectroscopic redshift is found on the Rainbow database but on the T07's sample (37 galaxies) we use the values of redshift and stellar masses from that catalog. c) Finally, if no spectroscopic redshift is found in any of the two catalogs we have used only those objects where the photometric redshift determination is robust (317 objects). This means that we have compared the two independent photo-z estimations found in T07 and Barro et al. (2011a) and we have only taken those objects where the photometric redshifts disagree less than $\Delta z_{\text{phot}} = 0.070$ for $0.0 < z < 0.5$, $\Delta z_{\text{phot}} = 0.061$ for $0.5 < z < 1.0$, and $\Delta z_{\text{phot}} = 0.083$ for $1.0 < z < 2.5$ (typical quality of the photo-z's in the Rainbow catalog in EGS obtained by comparing them with spec-z's, Barro et al. 2011b). This removes 94 galaxies. For consistency with the sample of satellite galaxies, for these 317 objects we take the stellar masses and photometric redshift from the Rainbow catalog. After this selection, the number of objects in the final sample of massive galaxies is 694, of which 317 have photometric redshifts from Rainbow and 377 have spectroscopic redshifts (340 from the Rainbow catalog and 37 from T07).

A final cut in the number of galaxies of our main sample is required to assure that the fraction of galaxies with satellites along our explored redshift range is not biased by the stellar mass completeness limit of the Rainbow database. The stellar mass limit (75% complete) of the Rainbow database at each redshift is provided in Pérez-González et al. (2008, see their Fig. 4). In the redshift range $0 < z < 2$ we have selected only those massive galaxies whose stellar masses are 10 times larger than the completeness limit at each redshift. There are 629 galaxies (with a mean stellar mass

¹ https://rainbowx.fis.ucm.es/Rainbow_Database/

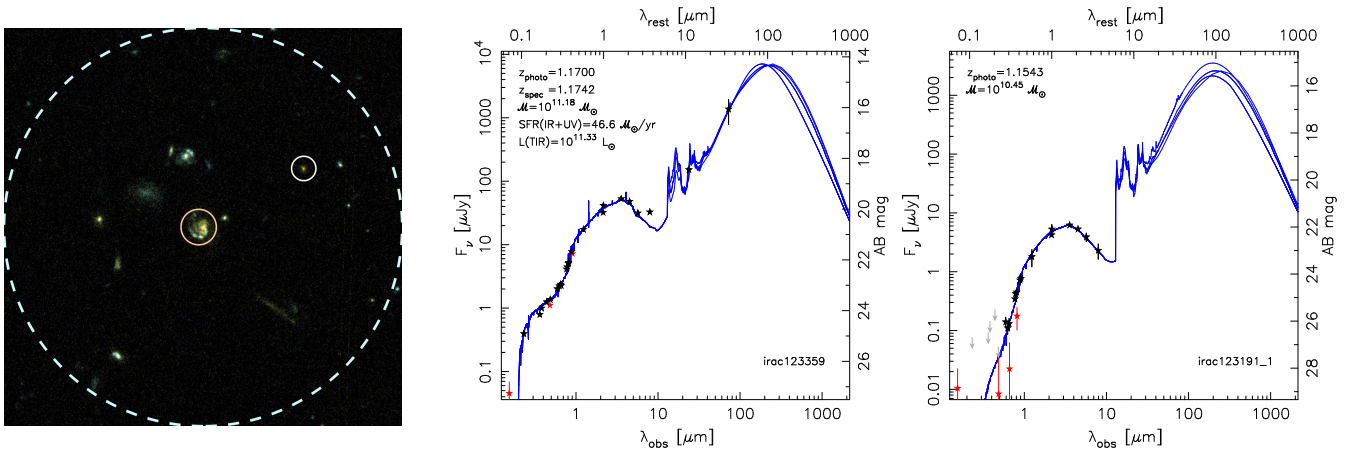


Figure 2. : *Left panel:* ACS color image of the massive galaxy IRAC123359 (in the centre) at $z = 1.17$ with a satellite galaxy (IRAC123191-1) that meets the selection criteria used in this work enclosed by a white circle. A circle of radius 100 kpc is plotted with a dashed line. *Central and right panels:* Spectral energy distributions for both the massive (central panel) and the satellite (right) galaxies. These panels also include the redshift and stellar mass estimates according to the Rainbow database.

of $M = 1.3 \times 10^{11} M_{\odot}$ for this sample) that meet these criteria. On doing that we are secure that we can explore within the Rainbow catalog satellites down to 1:10 mass ratio of the central galaxy in the range $0 < z < 2$. For the same reason, this exercise is done up to $z = 1$ but this time only selecting those central galaxies with a stellar mass 100 times above the mass limit. This cut leaves us in the redshift range $0 < z < 1$ with 194 massive galaxies (with a mean stellar mass of $M = 1.7 \times 10^{11} M_{\odot}$). The stellar masses and the redshifts for the central galaxies studied in this work are illustrated in Fig. 1.

3 SELECTION CRITERIA

To identify the satellite galaxies around our central objects we have applied the following procedure: (1) we identify all the galaxies in the Rainbow catalog which are within a projected radial distance to our central galaxies of $R_{\text{search}}=100$ kpc (corresponding to 0.3 and 0.2 arcmin for $z = 0.5$ and $z = 2$, respectively); (2) the difference between their photometric redshifts and the redshift of the central galaxies is lower than the 1σ uncertainty in the estimation of the photometric redshifts of the Rainbow database (i.e., $\Delta z_{\text{phot}} = 0.070$ for $0 < z < 0.5$, $\Delta z_{\text{phot}} = 0.061$ for $0.5 < z < 1$, and $\Delta z_{\text{phot}} = 0.083$ for $1 < z < 2.5$); and (3) the stellar mass of these objects should be within $0.1 < M_{\text{sat}}/M_{\text{central}} < 1.0$ for the galaxies in the range $0 < z < 2$, and within $0.01 < M_{\text{sat}}/M_{\text{central}} < 1.0$ for the galaxies in the range $0 < z < 1$. An example of satellite galaxy satisfying the above criteria is shown in Fig. 2. Finally, we consider different redshift bins (see Table 1) to explore the evolution of the fraction, F_{sat} , of massive galaxies with satellites. The width of these bins were chosen to include a similar number of massive galaxies in each bin and have a similar statistics among them.

We adopted a search radius of 100 kpc. This radius is a compromise between having a large area for finding a significant number of satellite candidates that are gravitationally bound to our central massive galaxies but not as large as to be severely contaminated by background objects. In any case, we have explored what is the effect on our measurements if we select larger radii of exploration. We computed the fraction of massive galaxies with satellites for different search radii ($R_{\text{search}}=100, 150, 200$ and 250 kpc). The results of this experiment in the mass range $0.1 < M_{\text{sat}}/M_{\text{central}} < 1$ are

shown in Fig.3. The numbers presented here are corrected of background contamination as it will be explained later. As it is expected, we detect an increasing number of massive galaxies with satellites as we expand the search radius R_{search} . The only exception is the redshift range $1.1 < z < 2.0$ where the fraction of massive galaxies with satellites is constant within the error bars. It is worth noting that, in general, beyond $R_{\text{search}}=150$ kpc there is not a net increase in the fraction of massive galaxies with satellites. Moreover, our results are basically unchanged if we use a search radius of 100 kpc or 150 kpc. For this reason, on what follows we will present the results based on a search radius of 100 kpc as our simulations show that this case is affected by the background contamination a factor of ~ 2 less than the 150 kpc case.

Similarly to the selection of the search radius, we have restricted our potential satellite galaxies to have a redshift difference with the central galaxy not larger than the 1σ uncertainty in the estimation of the photometric redshifts of the Rainbow database. Larger redshift differences could be used to include more potential candidates but this is transformed also into a larger background contribution to our measurements. For instance, we estimated how the fraction of massive galaxies with satellites changed when using 2σ uncertainty in the estimation of the photometric redshifts instead of 1σ . As expected, we found a slight increase ($\lesssim 30\%$) on the fraction but also our error bars increased (by a 50%) by the larger amount of background contamination. As these change do not alter our main results but increase our error bars, we have used the 1σ criteria explained in this paper.

3.1 Background estimation

Despite we have used photometric redshift information to select our potential satellite galaxies, there is still a fraction of objects that satisfy the above criteria but are not gravitationally bound to our massive galaxies. These objects are counted as satellites because the uncertainties on their redshift estimates include them within our searching redshift range. These foreground and background objects (hereafter we will use the term background to refer to both of them) constitute the main source of uncertainty in this kind of studies. Consequently, it is key to estimate accurately the background contamination in order to statistically subtract its contribution from the fraction of galaxies with observed satellites.

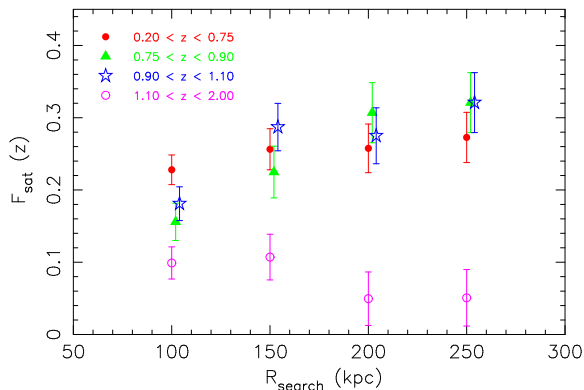


Figure 3. Fraction of massive galaxies having satellites within different projected radial distances (search radius, R_{search}) in the mass range $0.1 < M_{\text{sat}}/M_{\text{central}} < 1.0$ for the different redshift bins studied in this work.

To estimate the fraction of background sources that contaminates our satellite samples we have run a set of simulations. This method consists on placing a number of mock massive galaxies (equal to the number of our central galaxies) randomly through the volume of the catalog. To match our observed redshift distribution we assure that in our simulations, the number of mock galaxies that are within each redshift bin is the same than in our observed sample. Once we have placed our mock galaxies through the catalog, we count which fraction of these mock galaxies have satellites around them taking into account our criteria of redshift and distances explained above. This procedure is repeated two million times to have a robust estimation of the fraction of mock galaxies with satellites. We call this average fraction S_{simul} . Additionally, these simulations allowed us to estimate the scatter in the fraction of galaxies that have contaminants. We use this scatter as an estimation of the error of our real measurements. We consider then this fraction to be representative of the background affecting our real central sample. The galaxies in our mock samples keep fixed the parameters of the massive galaxies (i.e., stellar masses and Sérsic indices).

Taking into account that the observed fraction of galaxies with satellites, F_{obs} , is the sum of the fraction of galaxies with real satellites, F_{sat} , plus the fraction of galaxies which have not satellites but are affected by contaminants $(1 - F_{\text{sat}}) \times S_{\text{simul}}$ we arrive to the following expression:

$$F_{\text{sat}} = \frac{F_{\text{obs}} - S_{\text{simul}}}{1 - S_{\text{simul}}}. \quad (1)$$

The results of our simulations are shown in Table 1. From these simulations we see that the fraction S_{simul} of massive galaxies we expect to be contaminated by false satellites (using our searching criteria) is $\sim 10\%$ for $0.1 < M_{\text{sat}}/M_{\text{central}} < 1.0$ and $\sim 25\%$ for $0.01 < M_{\text{sat}}/M_{\text{central}} < 1.0$.

3.1.1 Clustering effects

It is well known that massive galaxies, particularly in the nearby Universe, tend to populate regions which are overdense compared to the average density of the Universe. This implies that there is an excess of probability (which we will term as clustering) of finding galaxies that could be misidentified as satellites of our main targets. It is worth noting that this probability excess is not related to the accuracy of our redshift estimations. Even with all the redshifts measured spectroscopically, the effect of clustering will be equally

relevant in our estimates as this effect is inherent to our inability of measuring real distances but distances inferred by recessional velocities. In massive cluster of galaxies, with velocity dispersion of $\sim 1000 \text{ km s}^{-1}$, this will limit our accuracy on estimating real galaxy associations.

Being the clustering a local effect, ideally one would like to measure its influence as closer as possible to the central galaxy. In practice, this is done by measuring the amount of satellite candidates in different annuli beyond our search radius (Chen et al. 2006; Liu et al. 2011). We will call to the fraction of massive galaxies having satellites in these annuli as S_{cluster} . This fraction measures both the effect of the background contamination plus the excess over this background due to the clustering. This method has the disadvantage, compared to the simulations that we have conducted above, that is statistically more uncertain. S_{cluster} can be measured only around our massive galaxies and this number is relatively small. For this reason, S_{cluster} is determined with an error larger than S_{simul} . We count the satellites in 9 different annuli in the radial range $100 < R < 330 \text{ kpc}$ (the size of each annuli was selected to contain the same area than the searching area within 100 kpc). We find, as expected, that the number of satellites decreases in the outer annuli, reaching asymptotically (within the errors) the values we get using the first background estimation method. However, in general, and particularly for the lower redshift bins, the number of detected satellites is higher for the inner annuli than in the random case, and therefore, the clustering is not negligible. As we noted before, the detection of satellites does not increase at $R_{\text{search}} > 150 \text{ kpc}$. For this reason, and as a compromise between proximity to the massive galaxies and having enough statistics, we have used the average detections of satellites in the two annuli closer to $R=150 \text{ kpc}$ ($173 < R < 200 \text{ kpc}$ and $200 < R < 224 \text{ kpc}$) to estimate the effect of the clustering. The uncertainty at measuring S_{cluster} is not straightforward to calculate and we have decided to estimate that value summing quadratically the background uncertainty measured in the simulations estimating S_{simul} plus the dispersion between the two different radial annuli used in the clustering determination.

The significance of the clustering is quantified in Table 1. We find that above $z > 1$ the clustering is playing a minor role as S_{cluster} and S_{simul} are very much alike within the errors. However, at $z < 1$, $S_{\text{cluster}} \sim 1.5 \times S_{\text{simul}}$. As it is expected, the effect of the clustering is more relevant at lower redshifts. At high redshifts, the overdensities are less significant as the large scale structures would be still not completely formed.

4 RESULTS

In Table 1 we summarize the results obtained in this work. For each redshift bin, we present the fraction of galaxies with satellites initially found for our sample of massive galaxies, F_{obs} , the background estimate S_{simul} derived from the mock catalogues, and the final fraction of massive galaxies with satellites, F_{sat} , after the correction of the background contamination with Eq. 1. The associated errors correspond to the standard deviation from the measurements obtained in the mock catalogues as explained in the previous section. In addition, we include the expected contamination due to the clustering estimate, S_{cluster} , and the fraction of massive galaxies with satellites after this correction F_{cluster} .

Our results are also illustrated in Fig. 4. Our main result is seen in the upper left panel of Fig. 4: the fraction of massive galaxies with satellites, within a projected radial distance of 100 kpc, in the range $0.1 < M_{\text{sat}}/M_{\text{central}} < 1$ remains basically constant ($17 \pm 3\%$)

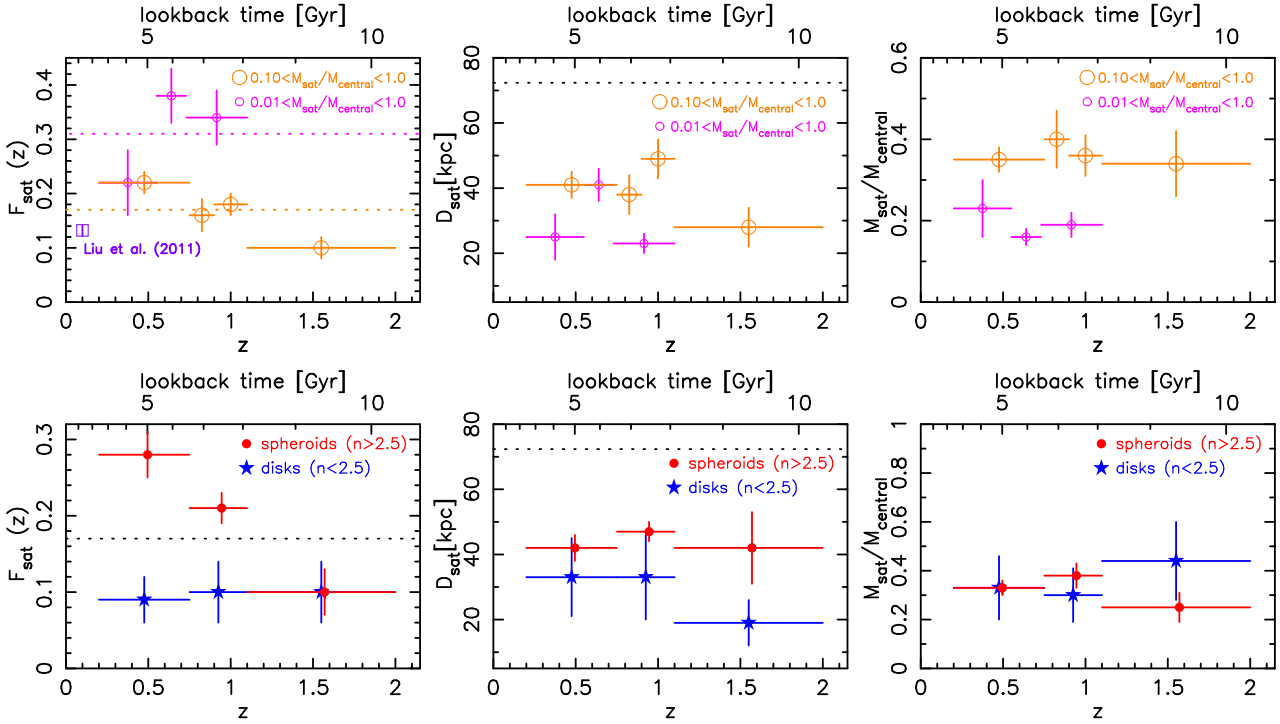


Figure 4. Fraction of massive galaxies having satellites (and their properties) within a projected radial distance of 100 kpc for different redshift bins. Upper panels show the fraction of massive galaxies with satellites in the mass range $0.1 < M_{\text{sat}}/M_{\text{central}} < 1.0$ (orange dots) and the fraction of massive galaxies with satellites in the mass range $0.01 < M_{\text{sat}}/M_{\text{central}} < 1.0$ (magenta dots). In the bottom panels, we explore the fraction of massive galaxies with satellites in the mass range $0.1 < M_{\text{sat}}/M_{\text{central}} < 1.0$ when our sample is split depending on the Sérsic index (morphology) of the galaxies (red dots for $n > 2.5$ -spheroids- and blue stars for $n \leq 2.5$ -disks). The horizontal dotted lines in the upper left panel correspond to the average fitted values to our findings. *Central panels:* Mean projected distances where the satellites are found after statistical correction of the background. The dashed line indicates the average projected distance obtained for mock satellites in the simulations (i.e. this is the expected distance if the satellites were an artifact of the background contamination). *Right panels:* Mean mass ratios between the satellites and their massive galaxies. The horizontal bars indicate the range of redshifts considered for each measurement. For clarity, we have slightly shifted the data corresponding to the spheroids-like objects.

in the redshift interval $0 < z < 2$. To have a $z = 0$ comparison, we have added the measurement from Liu et al. (2011) using the SDSS sample. They find that at $z = 0$ the fraction of massive galaxies with satellites in the mass range and projected radius explored here is very similar. In the same panel, we show the same analysis up to $z = 1$ for satellite galaxies with $0.01 < M_{\text{sat}}/M_{\text{central}} < 1.0$. Although a little bit noisier due to the lower statistics, our findings agree with a relative constant fraction ($31 \pm 6\%$) of massive galaxies having such type of satellites.

Our sample of massive galaxies is large enough that we can explore whether the fraction of massive galaxies with satellites in the range $0.1 < M_{\text{sat}}/M_{\text{central}} < 1$ depends on the morphology of the massive galaxy. We have used the Sérsic index as a proxy to the galaxy morphology. In the nearby universe, galaxies with $n < 2.5$ are mostly disc-like objects, whereas galaxies with $n > 2.5$ are mainly spheroids (e.g., Andreidakis et al. 1995; Blanton et al. 2003; Ravindranath et al. 2004). We have used the published Sérsic indexes provided by T07 to separate our galaxies. We illustrate our results in the bottom left panel of Fig. 4. There is a hint that massive galaxies with spheroid-like morphologies tend to have a larger fraction (a factor of 2-3) of galaxies with satellites than disk-like massive objects. This result is more prominent at low redshift where the clustering of the massive spheroid population could be an issue.

We can repeat the same exercise but this time using the clustering correction (which contains also the background effect) to explore how our results depend on this effect. The comparison between the two types of corrections are shown in Fig. 5. In general,

the correction due to the clustering decreases the fraction of massive galaxies which contains satellites. This is now $12 \pm 2\%$ in the redshift interval $0 < z < 2$ for $0.1 < M_{\text{sat}}/M_{\text{central}} < 1$ and $23 \pm 4\%$ for $0.01 < M_{\text{sat}}/M_{\text{central}} < 1.0$ up to $z = 1$.

4.1 Robustness of the results

The results presented in this paper are the product of combining two different datasets: the T07 sample of massive galaxies and the Rainbow catalogue. In addition, we have used photometric redshifts and, when available (54% of the time), spectroscopic redshifts. We have checked how robust are our results to the use of more homogeneous dataset, as using only a sample of massive galaxies with spectroscopic redshifts or, to base our full analysis only on the Rainbow database.

In our first test, we used only the central galaxies in our sample with spectroscopic redshifts and counted which fraction has satellites following the same procedure explained above and after correcting for the background. The width of the redshift bins for this sample were again chosen to include a similar number of massive galaxies and have a similar statistics to compare with the other samples. The output of this test is shown in Fig. 6. We get, for the case of $0.1 < M_{\text{sat}}/M_{\text{central}} < 1$ up to $z = 2$, an average fraction of $19 \pm 4\%$. It can be seen that this result is in full agreement with our previous estimation for this quantity. In a second test, we have taken the redshifts and stellar masses only from the Rainbow catalog to check whether there are systematic effects due to the use of com-

Table 1. Fraction of massive galaxies with satellites at different redshifts. For each redshift range we present the number of massive galaxies N_{central} in each bin (number of galaxies with spectroscopic redshifts in brackets), the observed fraction of massive galaxies with satellites F_{obs} , the estimate of the background contamination S_{simul} , and the estimate of the clustering effect S_{cluster} . Finally, we present the final fraction of massive galaxies with satellites when i) the correction for the background contamination (F_{sat}) or ii) the clustering effect (F_{cluster}) is applied.

Redshift range	N_{central} (N with spec z)	F_{obs}	S_{simul}	S_{cluster}	F_{sat}	F_{cluster}
All galaxies						
$0.10 < M_{\text{sat}}/M_{\text{central}} < 1.00$						
$0.20 < z < 0.75$	197 (130)	0.29	0.09 ± 0.02	0.15 ± 0.02	0.22 ± 0.02	0.17 ± 0.02
$0.75 < z < 0.90$	129 (76)	0.24	0.10 ± 0.03	0.17 ± 0.03	0.16 ± 0.03	0.08 ± 0.03
$0.90 < z < 1.10$	142 (99)	0.25	0.08 ± 0.02	0.13 ± 0.03	0.18 ± 0.02	0.13 ± 0.02
$1.10 < z < 2.00$	161 (55)	0.18	0.09 ± 0.02	0.09 ± 0.03	0.10 ± 0.02	0.10 ± 0.02
$0.01 < M_{\text{sat}}/M_{\text{central}} < 1.00$						
$0.20 < z < 0.55$	51 (40)	0.37	0.20 ± 0.06	0.24 ± 0.06	0.22 ± 0.06	0.16 ± 0.06
$0.55 < z < 0.73$	70 (42)	0.53	0.24 ± 0.05	0.36 ± 0.05	0.38 ± 0.05	0.28 ± 0.05
$0.73 < z < 1.10$	73 (53)	0.52	0.27 ± 0.05	0.36 ± 0.06	0.34 ± 0.05	0.25 ± 0.06
Spheroid – like ($n > 2.5$) galaxies						
$0.10 < M_{\text{sat}}/M_{\text{central}} < 1.00$						
$0.20 < z < 0.75$	137	0.34	0.09 ± 0.03	0.16 ± 0.03	0.28 ± 0.03	0.23 ± 0.03
$0.75 < z < 1.10$	176	0.27	0.08 ± 0.02	0.14 ± 0.04	0.21 ± 0.02	0.15 ± 0.04
$1.10 < z < 2.00$	85	0.18	0.08 ± 0.03	0.08 ± 0.03	0.10 ± 0.03	0.10 ± 0.03
Disk – like ($n < 2.5$) galaxies						
$0.10 < M_{\text{sat}}/M_{\text{central}} < 1.00$						
$0.20 < z < 0.75$	60	0.18	0.10 ± 0.03	0.15 ± 0.04	0.09 ± 0.03	0.05 ± 0.04
$0.75 < z < 1.10$	95	0.19	0.09 ± 0.03	0.16 ± 0.04	0.10 ± 0.04	0.04 ± 0.04
$1.10 < z < 2.00$	76	0.18	0.09 ± 0.04	0.09 ± 0.05	0.10 ± 0.04	0.11 ± 0.05

binning different samples. We get, in this case, a fraction of $17 \pm 2\%$. Again, this result agrees perfectly with the original estimate. We conclude, accordingly, that our results are robust to both the use of spectroscopic redshifts only and to the mixing of different datasets.

Another test that we have conducted is to check whether our results are robust to a change in the stellar mass limit at selecting our massive galaxies. As it is illustrated in Fig. 1, the galaxies at higher redshifts are slightly more massive than the bulk of objects at lower redshift to guarantee that we can study satellites above a given mass ratio along the full redshift range. We have checked how our results change if we select only massive galaxies with stellar masses above $2 \times 10^{11} M_{\odot}$. We have done this exercise for the case $0.1 < M_{\text{sat}}/M_{\text{central}} < 1$ up to $z = 2$. With the new mass limit, we get an average fraction of $\sim 23\%$. This is in good agreement with our original estimation for this fraction. Again, increasing the stellar mass limit does not alter substantially the fraction of massive galaxies with redshift.

4.2 Properties of the satellite galaxies

In addition to counting which fraction of the massive galaxies have satellites, we can also estimate the average projected radial distances of these satellites and the average mass ratios between the satellites and the massive objects. To estimate these quantities properly, we need to correct statistically by the effect of the contaminants. This can be done using the following expression:

$$\langle Q_{\text{sat}} \rangle = \frac{F_{\text{obs}}}{F_{\text{sat}}} \langle Q_{\text{obs}} \rangle - \frac{S_{\text{simul}}}{F_{\text{sat}}} \langle Q_{\text{simul}} \rangle \quad (2)$$

where $\langle Q_{\text{obs}} \rangle$ is the observed mean value of the property Q (i.e. the projected radial distance or the mass ratio), $\langle Q_{\text{simul}} \rangle$ is the mean value obtained from the mock massive galaxies (i.e. the values that are found for the contaminants) and $\langle Q_{\text{sat}} \rangle$ is the value after the correction.

The mean projected radial projected distances (in kpc) of the satellites and their mean mass ratios $M_{\text{sat}}/M_{\text{central}}$ are compiled in Table 2 and shown in Fig. 4. We plot with a dashed line the average projected distance (~ 72 kpc) of the background galaxies detected as fake satellites in the simulations. After correcting by the effect of the contaminants, we find that our satellite galaxies are at a typical projected radial distance of ~ 40 kpc. This value is well below the expectation from a random distribution, suggesting that the satellites are gravitationally bounded to their central galaxies. This average distance seems to be pretty much independent (within the errors) of the satellite mass, the morphological type of the central galaxy and the redshift of the system.

Finally, we show in the right panels of Fig. 4 the mean mass ratio $M_{\text{sat}}/M_{\text{central}}$ in each redshift bin after the statistical correction. We find that M_{sat} is around $0.36 M_{\text{central}}$ when we explore satellite galaxies within a mass ratio of $0.1 < M_{\text{sat}}/M_{\text{central}} < 1$ (this value is 0.28 when we use the clustering correction). If we explore down to a mass ratio of 0.01 then M_{sat} is around $0.15 M_{\text{central}}$ (0.14 correcting by the clustering effect). It is worth noting that in both cases, the mean masses of our satellites are over $10^{10} M_{\odot}$ and consequently we are detecting satellites with large masses. When we split the sample depending on their Sérsic indices (bottom right panel in Fig. 4), there are not significant differences, within the errors, between both samples. Again we find that the satellites of massive galaxies are

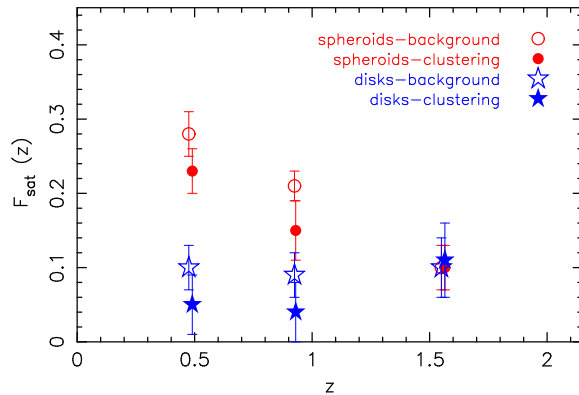
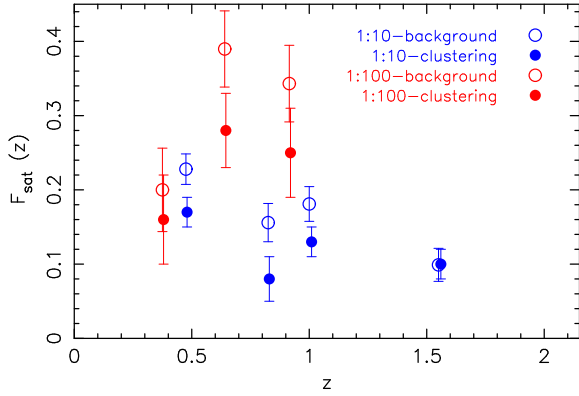


Figure 5. Fraction of massive galaxies with satellites after correction with the background contribution computed from the simulations (open symbols) and when the clustering estimation is used (filled symbols). *Top panel:* The fraction of massive galaxies with satellites is separated in two groups: $0.1 < M_{\text{sat}}/M_{\text{central}} < 1.0$ (blue triangles) and $0.01 < M_{\text{sat}}/M_{\text{central}} < 1.0$ (red squares). *Bottom panel:* Fraction of massive galaxies in the mass range $0.1 < M_{\text{sat}}/M_{\text{central}} < 1.0$ depending on the Sérsic index (morphology) of the central galaxies.

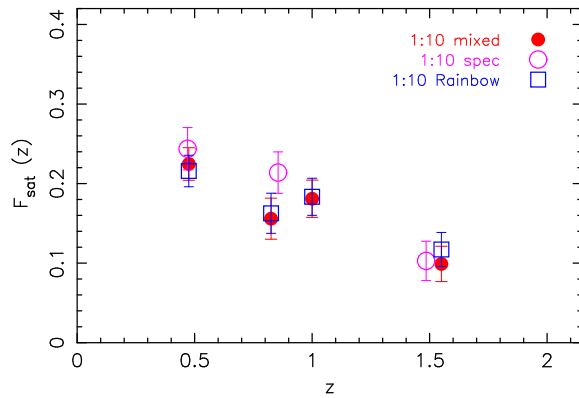


Figure 6. Testing the robustness of the fraction of massive galaxies with satellites in the mass range $0.1 < M_{\text{sat}}/M_{\text{central}} < 1.0$ for different datasets: our original sample described in Sect. 2 (red points), a purely spectroscopic sample (magenta circles) and a sample based only on the Rainbow catalogue (blue squares).

Table 2. Mean projected radial distances between the satellites and the central galaxies and their mean mass ratios ($M_{\text{sat}}/M_{\text{central}}$). These values correspond to the case where only the background correction has been applied.

Redshift range	Radial Distance (kpc)	$M_{\text{sat}}/M_{\text{central}}$
All galaxies		
$0.10 < M_{\text{sat}}/M_{\text{central}} < 1.00$		
$0.20 < z < 0.75$	41 ± 4	0.35 ± 0.03
$0.75 < z < 0.90$	38 ± 6	0.40 ± 0.07
$0.90 < z < 1.10$	49 ± 6	0.36 ± 0.05
$1.10 < z < 2.00$	28 ± 6	0.34 ± 0.08
Spheroid-like ($n > 2.5$) galaxies		
$0.10 < M_{\text{sat}}/M_{\text{central}} < 1.00$		
$0.20 < z < 0.55$	25 ± 7	0.23 ± 0.07
$0.55 < z < 0.73$	41 ± 5	0.16 ± 0.02
$0.73 < z < 1.00$	23 ± 3	0.19 ± 0.03
Disk-like ($n < 2.5$) galaxies		
$0.10 < M_{\text{sat}}/M_{\text{central}} < 1.00$		
$0.20 < z < 0.75$	33 ± 12	0.33 ± 0.13
$0.75 < z < 1.10$	33 ± 13	0.30 ± 0.11
$1.10 < z < 2.00$	19 ± 7	0.44 ± 0.16

similar in their mean properties (distances and mass ratios) independently of the morphological type of their central galaxies and redshift.

5 DISCUSSION AND CONCLUSIONS

The results of this paper support a picture where the fraction of massive ($M_{\text{star}} \sim 10^{11} M_{\odot}$) galaxies with satellites, within a projected radius of 100 kpc, has not changed with time since $z \sim 2$. This fraction remains around $\sim 15\%$ for galaxies with satellites with mass $M_{\text{star}} \gtrsim 10^{10} M_{\odot}$ and around $\sim 30\%$ if we explore satellites with masses $M_{\text{star}} \gtrsim 10^9 M_{\odot}$ up to $z = 1$.

Interestingly, we find a hint that the fraction of massive galaxies with satellites is larger (a factor of around 2 to 3) for those galaxies with spheroid-like morphologies than for galaxies with disk-like appearance (much evident for $z \lesssim 1.1$). This fact could be linked to the different size growth we observe for these two types of objects as cosmic time increases. In fact, spheroid galaxies are known for growing more dramatically in size since $z \sim 3$ than disk galaxies (see e.g., T07 Buitrago et al. 2008). It could be also possible that the fraction of satellites difference between spheroid and disk-like galaxies would be just an effect of the clustering, more relevant at lower redshifts (Sect. 3.1.1). However, this difference remains even when this effect is taken into account (Fig. 5). We remark, however, that it is difficult to correct the clustering effect accurately. With the present dataset, a mild redshift evolution of the fraction of spheroid-like galaxies with satellites can not be excluded.

Due to the enormous uncertainty on the merging timescales (e.g., Lotz et al. 2011), it is beyond the scope of this work to estimate a robust merger rate associated to our measurements.

Nonetheless, we can make a crude estimation on the number of mergers a massive galaxy experiences since a given z according to the following expression: $N_m = T(z) \times F_{\text{sat}}/\tau_m$, where $T(z)$ is the interval of cosmic time since a given z to now, and τ_m is the merging timescale of the satellite within a given radius. For each massive galaxy at $z = 2$ and assuming $\tau_m \sim 1.5$ Gyr (e.g. Lotz et al. 2011), we would expect that the number of mergers with mass ratio around 1:3 would be ~ 1 (~ 2 in the case of an spheroid-like galaxy) since that epoch. For a massive galaxy at $z = 1$, we would expect that the number of mergers with mass ratio around 1:6 would be ~ 1.5 since that redshift. Again, these numbers are uncertain and very much dependent on the exact merging timescale which is a function of the baryonic mass ratio and the model used to estimate this quantity (e.g., Bluck et al. 2009; Conselice et al. 2009; Lotz et al. 2011; Man et al. 2011). These numbers of mergers, however, are slightly lower (although the exact amount is difficult to quantify) than the expected number of mergers obtained using theoretical recipes for the size increase of a galaxy after a merger (see Trujillo et al. 2011). Recently, Bluck et al. (2011) find that a massive galaxy ($M_{\text{star}} > 10^{11} M_{\odot}$) will experience on average $N_m = (1.1 \pm 0.2)/\tau_m$ minor mergers over the redshift range $z = 1.7 - 3$. This would mean a final $N_m \sim 1$ using the τ_m considered in our work. If this is confirmed, it will point out to the possibility that the merging activity at those redshifts would be higher than at lower redshifts. When extrapolated in redshift, they find a total final number of minor mergers of $N_m = (4.5 \pm 2.9)/\tau_m$ from $z = 3$, although once more, the large errors make very uncertain to constrain the final number of experienced mergers.

At present, there are a few cosmological simulations where the size growth of the massive galaxies is explained by the accretion of minor satellites (see Naab et al. 2009; Oser et al. 2011). It would be straightforward to compare our findings with those cosmological simulations of galaxy formation and check whether the fractions that we find are recovered in such theoretical analysis. If this was the case, the support to the minor merging mechanism as the main responsible for the size evolution of the massive galaxies will be greatly enhanced.

ACKNOWLEDGMENTS

We thank the anonymous referee for a careful and constructive reading of the manuscript that help us to improve the quality of the paper. Authors are grateful to Lulu Liu for providing us with their measurements of the fraction of galaxies with satellites obtained from the SDSS, used here as a local ($z = 0$) comparison. We thank Juan Betancort for his valuable input on several aspects of the statistical analysis of this paper. We are devoted to Sergio Pascual for his very useful help in programming questions. We would like also to acknowledge fruitful discussions with Javier Cenarro, Luis Díaz, Rosa Domínguez, Cesar González, Carlos López-San Juan, José Oñorbe, Thorsten Naab and Vicent Quilis. IT is a Ramón y Cajal Fellow of the Spanish Ministry of Science and Innovation. This work has been supported by the “Programa Nacional de Astronomía y Astrofísica” of the Spanish Ministry of Science and Innovation under grant AYA2010-21322-C03-02. PGP and GB acknowledge support from the Spanish Programa Nacional de Astronomía y Astrofísica under grants AYA2009-10368 and AYA2009-07723-E. This work has made use of the Rainbow Cosmological Surveys Database, which is operated by the Universidad Complutense de Madrid (UCM).

REFERENCES

- Andredakis, Peletier, Balcells, 1995, MNRAS, 275, 874
 Barro G., Pérez-González P. G., et al., 2011, ApJS, 193, 13
 Barro G., Pérez-González P. G., et al., 2011, ApJS, 193, 30
 Bezanson R., van Dokkum P. G., et al., 2009, ApJ, 697, 1290
 Blanton M. R., Hogg D. W., et al., 2003, ApJ, 594, 186
 Bluck A. F. L., Conselice J., et al., 2009, MNRAS, 394, 51
 Bluck A. F. L., Conselice J., et al., 1111.5662B
 Boylan-Kolchin M., Springel V., et al., 2010, MNRAS, 406, 896
 Buitrago F., Trujillo I., et al., 2008, ApJL, 687, L61
 Bundy K., Ellis R. S., et al., 2006, ApJ, 697, 1369
 Bundy K., Fukugita M., et al., 2009, ApJ, 651, 120
 Cappellari M., di Serego Alighieri S., et al., 2009, ApJL, 704, L34
 Carrasco, Conselice, Trujillo, 2010, MNRAS, 405, 2253
 Cenarro A. J., Trujillo I., 2009, ApJL, 696, L43
 Chabrier G., 2003, PASP, 115, 763
 Chen J., Kravtsov A. V., et al., 2006, MNRAS, 381, 962
 Chen J., 2008, AJ, 484, 347
 Conselice C. J., Bundy K., et al., 2007, MNRAS, 381, 962
 Conselice, Yang, Bluck, 2009, MNRAS, 394, 1956
 Daddi E., Renzini A., et al., 2005, ApJ, 626, 680
 Davis M., Faber S. M., et al., 2003, Proc. SPIE, 4834, 161
 de Ravel L., Le Fèvre O., et al., 2009, A&A, 498, 379
 de Ravel L., Kampczyk P., et al., 2011, 1104.5470
 Fan L., Lapi A., et al., 2010, ApJ, 718, 1460
 Fan L., Lapi A., et al., 2008, ApJL, 689, L101
 Hopkins P. F., Hernquist L., et al., 2009, ApJ, 691, 1424
 Khochfar S., Burkert A., 2006, AJ, 445, 403
 Longhetti M., Saracco P., et al., 2007, MNRAS, 374, 614
 Lotz J. M., Jonsson P., et al., 2011, ApJ, 742, 103
 Liu L., Gerke B. F., et al., 2011, ApJ, 733, 62
 López-Sanjuan C., Ballcells M., et al., 2010, ApJ, 710, 1170
 López-Sanjuan C., Le Fèvre O., et al., 2011, AJ, 530, A20
 Man A. W. S., Toft S., et al., 2012, ApJ, 744, 85
 Martinez-Manso J., Guzman R., et al., 2011, ApJ, 738, 22
 Naab T., Johansson P. H., Ostriker J. P., 2009, ApJL, 699, L178
 Newman A. B., Ellis R. S., et al., 2010, ApJL, 717, L103
 Newman A. B., Ellis R. S., et al., 2011, 1110.1637
 Nierenberg A. M., Auger M. W., et al., 2011, ApJ, 731, 44
 Oser L., Naab T., et al., 2012, ApJ, 744, 630
 Pérez-González P. G., Rieke G. H., et al., 2008, ApJ, 675, 234
 Ravindranath S., Ferguson H. C., et al., 2004, ApJL, 604, L9
 Sérsic J. L., 1968, Atlas de galaxias australes
 Trujillo I., Förster Schreiber N. M., et al., 2006, ApJ, 650, 18
 Trujillo I., Conselice C. J., et al., 2007, MNRAS, 382, 109
 Trujillo, Ferreras, de La Rosa, 2011, MNRAS, 938, 3903
 van Dokkum P. G., Brammer G., 2010, ApJL, 718, L73
 van de Sande J., Kriek M., et al., 2011, ApJL, 736, L9